INTL JOURNAL OF ELECTRONICS AND TELECOMMUNICATIONS, 2014, VOL. 60, NO. 3, PP. 225–231
Manuscript received August 6, 2014; revised September, 2014. DOI: 10.2478/eletel-2014-0028

Modifications of Range-Doppler Algorithm for Compensation of SAR Platform Motion Instabilities

Ievgen M. Gorovyi, Oleksandr O. Bezvesilniy, and Dmytro M. Vavriv

***Abstract*— Two modifications of the range-Doppler algorithm (RDA) have been proposed to solve problems of SAR platform motion instabilities. First, the multi-look processing based on the RDA with an extended Doppler bandwidth has been introduced for correction of radiometric errors. Second, the RDA has been modified to perform SAR image formation on short-time acquisition intervals to use it in a recently-developed local-quadratic map-drift autofocus (LQMDA) method. The performance of the methods is illustrated with experimental data obtained by airborne SAR systems.**

***Keywords*— synthetic aperture radar (SAR), range-Doppler algorithm (RDA), multi-look processing, image formation, radiometric errors, autofocus**

I. Introduction

SYNTHETIC aperture radar (SAR) is a well-known instrument for high-resolution imaging of the earth surface [1]-[4]. High range resolution is typically achieved by transmitting pulses with a linear frequency modulation [4]-[5]. High azimuth resolution is obtained by coherent processing of the received pulses during the movement of the SAR platform. The main advantages of such radar are its ability to form the high-resolution images by using a physically small antenna and its independence of weather conditions and illumination level.

In the last decade, the usage of light-weight aircrafts and UAVs as SAR platforms has become very popular due to the low exploitation cost and quick operational availability [6]-[7]. One of the existing difficulties in the SAR image formation from a light-weight platform is the unstable movement of the platform in real flight conditions [1]-[4]. In particular, the trajectory of the sensor may deviate significantly from a straight line and it should be measured with a high accuracy. Also, the orientation of the antenna beam may change with time considerably. Such flight instabilities if not being accounted properly lead to the image quality degradation, which appears as brightness variations and defocusing effects in the resulting SAR images [1], [8]-[9].

A number of different SAR data processing algorithms have been developed so far [1]-[4]. The range-Doppler algorithm (RDA) is one of the most widely used [4], [9]-[10]. The main advantages of the method are related with its computational efficiency and simplicity of implementation. However, the problem is that the SAR processing in this case is performed under the assumption that the real antenna orientation angles are constant and the trajectory of the sensor is measured with a very high precision. The above mentioned requirements are often not fulfilled in the real flight conditions.

In the paper, two novel modifications of the RDA are introduced. We show that this SAR algorithm can be efficiently used to solve the two above-described problems, in particular, for the compensation of the unstable real antenna beam orientation and for the estimation of the residual phase errors from the SAR data via autofocusing.

In Section II, the principles of the RDA and the multi-look processing in the range-Doppler domain are described. Section III contains the ideas of how the RDA can be applied for the compensation of an unstable antenna beam orientation and correction of the resulting radiometric errors in SAR images. The application of the specifically modified RDA in a recently-developed SAR autofocus algorithm is described in Section IV. The efficiency of the proposed solutions is illustrated by examples of SAR images obtained with a Ku-band and an X-band airborne SAR systems.

II. Principles of Range-Doppler Algorithm

In this section, main principles of the SAR image formation are briefly described and peculiarities of the SAR data processing in the range-Doppler domain are considered.

A. Principles of SAR image formation

The general task of any SAR processing algorithm is to focus the SAR data [2]-[4]. This processing can be considered as a two-dimensional compression of the backscattered signals. A basic block-scheme of a typical SAR processing algorithm is shown in Fig. 1.

After the range compression of the raw data [4]-[5], the range cell migration correction (RCMC) is applied [2]-[4]. The effect of the range cell migration is related with the fact that the distance from the particular target to the moving SAR platform changes with time. As a result, the backscattered signal migrates throw the adjacent range cells during the SAR platform motion. Thus, after the range compression, the azimuth signal of the particular point target will be concentrated along a so-called migration curve. The RCMC is accomplished as the interpolation step along this migration curve [4]. The next important step of the SAR processing is the azimuth compression, which is performed as a convolution of the backscattered signal with a reference function [2]-[4]. The reference function is calculated based on the SAR platform trajectory parameters and the antenna beam orientation, which should be carefully measured. The application of the above described steps allows to obtain the SAR image of the scene.

I.M. Gorovyi, O.O. Bezvesilniy and D.M. Vavriv are with the Institute of Radio Astronomy, Kharkiv, Ukraine, (e-mail: gorovoy@rian.kharkov.ua, obezv@rian.kharkov.ua, vavriv@rian.kharkov.ua).

B. SAR processing in the range-Doppler domain

The key differences between the SAR processing algorithms are related with the way how the RCMC and azimuth

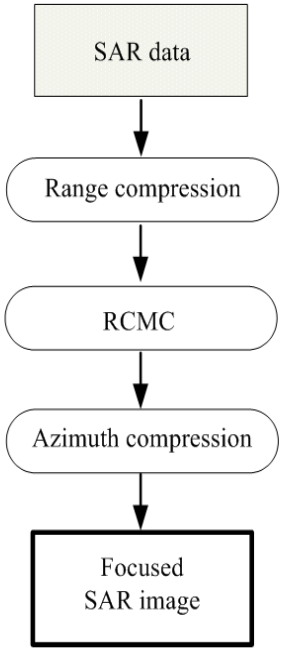

Fig. 1. Basic block-scheme of a typical SAR processing algorithm

compression are performed. The main advantages of the RDA are the possibility of the efficient RCMC in the range-Doppler domain and the aperture synthesis based on the usage of the fast Fourier transform (FFT) algorithm [4].

Fig. 2 illustrates how the RCMC is performed in the range-Doppler domain.

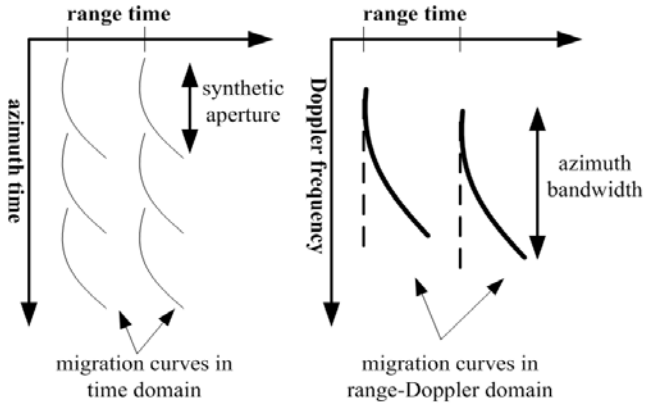

Fig. 2. Range migration curves in range-time and range-Doppler domains

In the left figure, six migration curves from the six point targets located at two ranges (3+3) are shown in the range-time domain. It is known that the point targets from the same range have similar migration curves shifted in azimuth according to the azimuth position of the targets. Since the target position within the real antenna beam is related with the Doppler frequency, all migration curves from the particular range gate will be combined into the single migration curve at this range in the range-Doppler domain [4] as shown in the right figure. After some straightforward mathematical derivations [4], one can find the equation for such migration curve in the range-Doppler domain:

$$R(f) = \frac{R\sqrt{1-\frac{\lambda^2 f_{DC}^2}{4V_X^2}}}{\sqrt{1-\frac{\lambda^2 f_D^2}{4V_X^2}}}, \quad (1)$$

where R is the slant range from the antenna phase center to the target when it crosses the center line of the antenna footprint, f_D is the azimuth (Doppler) frequency, λ is the radar wavelength, V_X is the reference velocity of the aircraft, f_{DC} is the mean Doppler frequency of the backscattered signal (the Doppler centroid). Thus, the RCMC processing can be performed for all targets at each given range simultaneously via the single interpolation along the migration curve (1) in the range-Doppler domain.

As for the azimuth compression, one can show that the reference function in the Doppler domain is determined by the following equations:

$$H(f,R) = \exp(i\varphi_C(f_D,R)),$$

$$\varphi_C(f_D,R) = \frac{4\pi R}{\lambda}\left(\sqrt{1-\frac{\lambda^2 f_D^2}{4V_X^2}}\sqrt{1-\frac{\lambda^2 f_{DC}^2}{4V_X^2}}+\frac{\lambda^2 f_D f_{DC}}{4V_X^2}\right). \quad (2)$$

The aperture synthesis in the RDA is performed via the phase correction in the range-Doppler domain using (2) followed by the inverse FFT.

The main assumption of the RDA is that the two-dimensional phase history function is separable – it can be represented as the product of two one-dimensional functions in the range-time domain [4], [10]. One refers to the range migration function and the other refers to the phase function. The problem is that this assumption does not hold in some cases, in particular, in the case of a large real antenna beam width or for high values of the squint angle. The existing azimuth and range phase cross-coupling effect influences the aperture synthesis performance and degrades the SAR image quality. It was shown [4] that such cross-coupling effect can be eliminated by the application of the additional phase compensation in the two-dimensional frequency domain as

$$H_{src}(f_D,f_R) = \exp(-j\varphi_{src}),$$

$$\varphi_{src}(f_D,f_R) = \pi\frac{f_R^2}{K_{src}(R_0,f_D)} = \frac{\pi}{2}\frac{\lambda^3 R_0 f_D^2 f_R^2}{v^2c^2\left(1-\frac{\lambda^2 f_D^2}{4V_X^2}\right)^{3/2}}, \quad (3)$$

where R_0 is the range of the closest approach, f_R is the range frequency, c is the speed of light.

C. Multi-look processing

Multi-look processing technique is commonly used for the suppression of the speckle noise [1]-[3]. This approach is based on the formation of several SAR images (SAR looks) of the same scene from different trajectory segments. The

obtained image sequence is then incoherently averaged resulting in a multi-look SAR image with the suppressed speckle noise and increased detailing level. In the frequency domain, the multi-look processing corresponds to the division of the whole processed Doppler bandwidth on the small

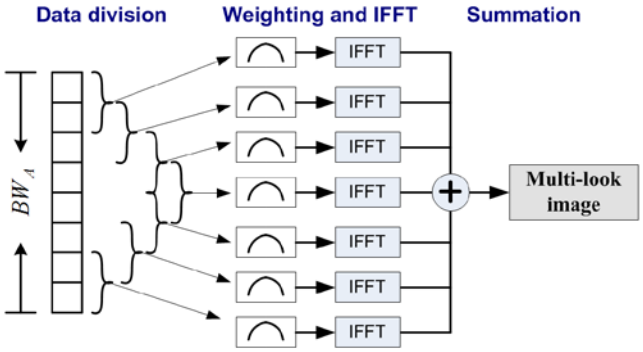

Fig. 3. Multi-look processing in the range-Doppler domain

sub-bands. The principle of the multi-look image formation in the range-Doppler domain is illustrated in Fig. 3 (the case of 7 half-overlapped SAR looks is considered).

After the phase correction step, which is performed for the whole Doppler spectrum, the Doppler sub-bands are independently weighted, and the inverse Fourier transforms are applied for all sub-bands providing the sequence of SAR images of the same scene. The length of a particular Doppler sub-band is determined by the required azimuth resolution:

$$BW(\rho_X) = K_w \frac{V_X}{\rho_X}, \tag{4}$$

where ρ_X is the azimuth resolution, K_w is the weighting window coefficient. The whole Doppler spectrum width is determined by the real antenna beam width θ_A as follows:

$$BW_A \approx \frac{2}{\lambda} V_X \theta_A . \tag{5}$$

Therefore, the number of the obtained SAR looks can be easily calculated as (for the half-overlapping scheme):

$$NL = \text{int}\left\{ \frac{BW_A}{BW(\rho_X)/2} \right\} - 1. \tag{6}$$

In the next section we will demonstrate how the multi-look processing in the range-Doppler domain can be used to compensate the existing real antenna beam orientation instabilities and correct the arising radiometric distortions.

III. Processing of Extended Doppler Bandwidth for Radiometric Correction

One of the existing problems in SAR imaging is the unstable orientation of the real antenna beam, which causes the radiometric (brightness) distortions in the obtained SAR images [9]. Actually, the initial assumption of RDA is constant real antenna beam orientation within a large data frame. Unstable motion of the SAR platform leads to situations when the directions of real antenna beam and calculated synthetic beams do not coincide. Fig. 4a illustrates this problem.

In such conditions a common RDA application leads to radiometric distortions in the obtained SAR images. In such conditions a common RDA application leads to radiometric distortions in the obtained SAR images.

It is known that the mean Doppler frequency of the backscattered signal depends on the antenna beam orientation angles α, β (pitch and yaw) as

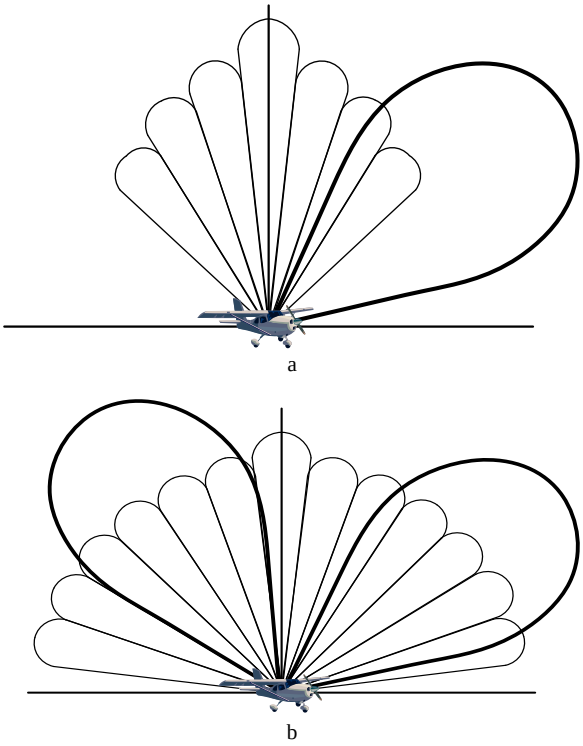

Fig. 4. Real antenna beam and synthetic beams (a – common multi-look processing, b – extended number of looks)

$$f_{DC} = \frac{2}{\lambda} \frac{x_R V_X}{R}, \tag{7}$$

where $x_R = H \tan\alpha \cos\beta + \sin\beta \sqrt{R^2 - \left(H/\cos\alpha\right)^2}$ is the azimuth position of a point on the Doppler centroid line at a slant range R, and H is the flight altitude. This means that the unstable antenna beam orientation leads to changes of the mean Doppler frequency of the backscattered signal.

Another important effect is related with the motion compensation procedure, which is commonly applied in the SAR processing for accounting the measured SAR platform trajectory [2]. It was shown [9] that the application of such procedure may lead to an additional broadening of the Doppler bandwidth. Thus, the total Doppler bandwidth BW_{Ext} can be written as

$$BW_{Ext} = BW_A + \Delta F_{DC}^{\alpha,\beta} + \Delta F_{DC}^{MoCo}, \tag{8}$$

where BW_A is the Doppler spectrum width corresponding to the real antenna beam width (5), $\Delta F_{DC}^{\alpha,\beta}$ is the broadening related with the unstable antenna beam orientation and ΔF_{DC}^{MoCo} is an additional broadening caused by the application of the conventional motion compensation procedure.

Therefore, in order to capture the SAR platform instabilities obtained extended Doppler bandwidth (8) should be used for the multi-look processing. Such multi-look processing is performed with the corresponding number of SAR looks (Fig. 4b)

$$NL_{Ext} = \mathrm{int}\left\{\frac{BW_{Ext}}{BW(\rho_X)/2}\right\} - 1. \qquad (9)$$

In this case some looks will be always within the real antenna beam.

An example of the dynamic Doppler spectrum calculated from the airborne SAR data is shown in Fig. 5.

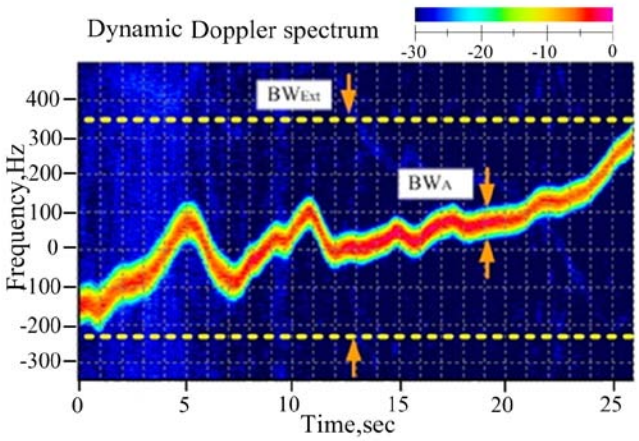

Fig. 5. Dynamic Doppler spectrum calculated from the real SAR data

Obviously, the extended Doppler bandwidth is several times larger than the actual width of the Doppler spectrum (5). Processing of the extended Doppler bandwidth in the range-Doppler domain allows to account the effects of the trajectory instabilities influence, in particular, the unstable antenna beam orientation and the consequences of the application of the conventional motion compensation procedure.

Since the unstable antenna beam orientation leads to a non-uniform scene illumination, it is necessary to correct the resulting brightness variations. We have developed a specific brightness correction procedure [11], which is based on the joint analysis of the obtained sequence of extended number of SAR looks and their smoothed low-frequency components.

Figure 6 illustrates how the developed radiometric correction procedure can be used with the range-Doppler algorithm. After the images formation with the RDA on the calculated extended Doppler bandwidth (8), the smoothed components of the SAR looks are built.

At this stage, the brightness estimation procedure is applied for these components followed by the construction of the composite images, which demonstrate the maximum brightness for each pixel. The final multi-look image is formed by the averaging of the constructed composite images based on the analysis of the smoothed components.

An example of the application of the proposed correction procedure is illustrated in Fig. 7. The illustrated SAR images were obtained by the Ku-band SAR system developed at the

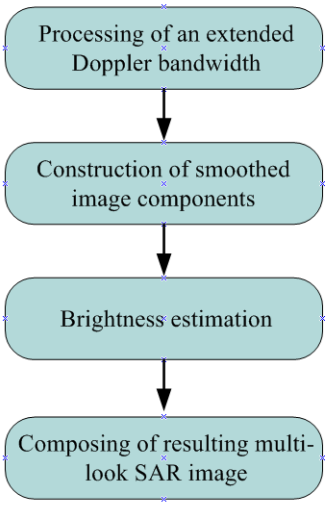

Fig. 6. Range-Doppler processing with extended number of looks for radiometric error correction.

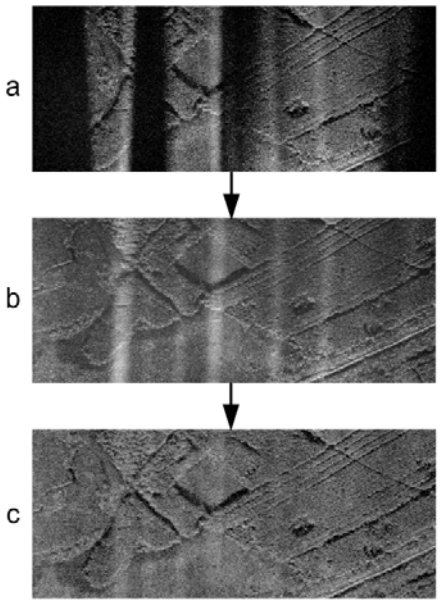

Fig. 7. Illustration of radiometric correction: (a) conventional multi-look RDA processing, (b) RDA processing with summation of extended number of looks, (c) multi-look image after radiometric correction.

Institute of Radio Astronomy [5]. The first SAR image (Fig. 7a) is obtained with the conventional RDA. One can observe significant radiometric distortions caused by the antenna orientation instabilities. The second SAR image (Fig. 7b) is the result of the non-coherent averaging of the SAR looks from the extended Doppler bandwidth. Some brightness variations exist due to the non-uniform scene illumination. Finally, the third SAR image (Fig. 7c) is an example of the application of the developed radiometric correction procedure. Obviously, the usage of range-Doppler algorithm with the proposed correction method allows to obtain SAR images without radiometric distortions.

IV. Local-Quadratic Phase Error Estimation and Modified Range-Doppler Processing

Another important problem in the SAR image formation is related with the precision of trajectory measurements [12]-[13]. In order to efficiently perform the aperture synthesis and obtain a well-focused SAR image of a scene it is necessary to know a precise platform position. A challenge is that the requirements for the trajectory measurements precision are often very high and even expensive navigation systems can not provide the necessary quality. As a result, uncompensated residual phase errors are inevitably left in the SAR data. These errors cause the strong defocusing effect in the obtained images of the ground surface [8].

The common solution in this case is the application of autofocus algorithms, which are based on the estimation of the phase error function directly from the radar signal. Recently we have shown that the estimates of the local quadratic phase errors on short-time intervals can be used for the reconstruction of an arbitrary residual phase error function [13]-[14]. The developed method is called the local-quadratic map-drift autofocus (LQMDA). The proposed algorithm is based on two key steps: the SAR processing on the short-time intervals with the local-quadratic phase error estimation and an arbitrary phase error reconstruction based on the local estimates. In order to estimate the local phase errors properly we have applied the modified version of the RDA adopted for such specific SAR processing.

The SAR processing on a short-time interval in the range-Doppler domain has several differences as compared to the conventional RDA [14]. First, in the conventional RDA, the reference function is built for the short Doppler sub-band determined by the required resolution as given by (4) and shown in Fig. 3. In the case of processing on the short interval, the signal from each point target on the scene will appear only on a small Doppler band. Therefore, in order to obtain the SAR image of the antenna footprint we should build the reference function for the whole Doppler bandwidth (5). Second important modification is related with the weighting window application. Obviously, the direct application of the weighting window to the whole Doppler spectrum will not weight the spectra of the individual point targets (Fig. 8). Therefore, the data collected on the short-time interval should be multiplied by the window $w_S(\tau)$ in the time domain before transformation into the frequency domain. In this way, the individual target spectra will be weighted properly.

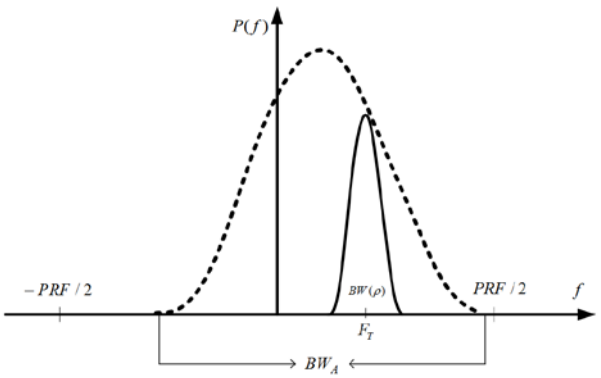

Fig. 8. SAR processing on a short-time interval in the range-Doppler domain

According to the introduced RDA modifications, two SAR images $I_{L,R}(t)$ built from the halves of the short-time interval (that are required for the autofocus estimation based on the map-drift principle) can be obtained as follows:

$$I_{L,R}(t) = \int_{-BW_A/2}^{BW_A/2} S_{L,R}(f) H^*(f) \exp[2\pi i f t] df \,, \quad (9)$$

where $S_L(f)$, $S_R(f)$ are the spectra of the SAR signals,

$$S_L(f) = \frac{2}{T_S} \int_{-T_S/2}^{0} w_S(\tau + T_S/4) s(\tau) \exp[-2\pi i f \tau] d\tau \,, \quad (10a)$$

$$S_R(f) = \frac{2}{T_S} \int_{0}^{T_S/2} w_S(\tau - T_S/4) s(\tau) \exp[-2\pi i f \tau] d\tau \,. \quad (10b)$$

The reference function in the Doppler domain is calculated as follows

$$H(f) = \int_{-T_A/2}^{T_A/2} w_H(t) h(t) \exp[-2\pi i f t] dt \,, \quad (11)$$

where $h(t)$ is the long reference function in the time domain, which is constructed from the navigation parameters, w_H is the window applied to limit the processed Doppler bandwidth (5), T_A is the length of the reference function. As a result, two highly overlapped images of the antenna footprint will be obtained for autofocusing.

It was shown, that in the case of presence of the local-quadratic phase error, the obtained SAR images will be defocused and shifted into the opposite directions [14]. One can perform the following approximation of described SAR images pair

$$|I_{L,R}(t)| = |\mathrm{sinc}[\pi\{F_{DR}(t - t_p) \pm \Delta F_{DR}^E (T_S/4)\}(T_S/2)]| \,, \quad (12)$$

where ΔF_{DR}^E is a local quadratic phase error coefficient, t_p is the azimuth position of a target. Using the obtained approximations a parameter F_{DR}^E can be determined as follows

$$\Delta F_{DR}^E = \frac{2\Delta t_{\max} F_{DR}}{T_S} \,, \quad (13)$$

where $\Delta t_{\max}$ is a linear shift, which can be estimated via cross-correlation of SAR images pair. In order to obtain the precise position of the cross-correlation peak several image preprocessing steps should be performed. In particular, local centering and normalization. This allows to enhance the contrast features and balance the contributions from different image parts. After the estimation of the cross-correlation peak position, the value of the local-quadratic phase error (13) is calculated. It should be emphasized that the proper SAR image synthesis using the modified RDA allows to perform the above described local estimation.

Second key step of the developed autofocus algorithm includes the reconstruction of an arbitrary residual phase error from the extracted local estimates. Fig.9 illustrates the overall scheme of the proposed LQMDA.

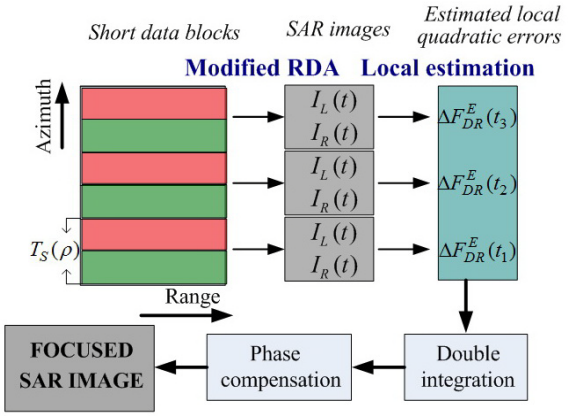

Fig. 9. Block-scheme of LQMDA

The block-scheme of the SAR processing with the incorporated LQMDA is illustrated in Fig. 8.

At first, the received raw data are compressed in range and the 1st-order (range-independent) motion compensation is applied. Then, the range cell migration correction (RCMC) is performed in the range-Doppler domain. After that, the 2nd-order (range-dependent) motion compensation is accomplished. At the next step the developed autofocus algorithm is applied for the estimation of the residual phase error function.

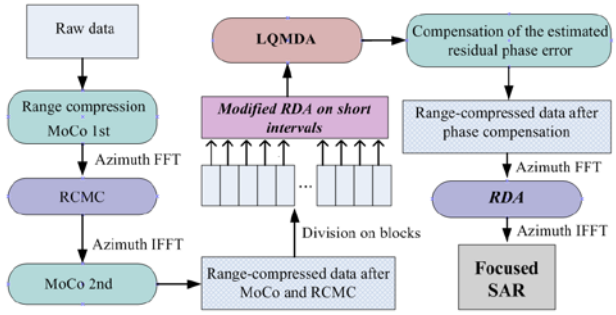

Fig. 10. Block-scheme of the SAR processing with developed autofocus method

After division of the SAR data into a sequence of the azimuth blocks the modified range-Doppler algorithm adopted for such SAR processing is applied to build the pair of SAR images. After that the linear shift between the images is measured to extract the value of the local-quadratic phase error. The local estimates on the short-time intervals provide the time-series of the local-quadratic phase errors, which is used to reconstruct the unknown residual phase error function. This function is then compensated in the SAR data and the conventional RDA is applied for the whole SAR data frame resulting in the well-focused SAR image.

The developed autofocus algorithm has been tested on the real SAR data obtained by the X-band SAR system [7] developed at the Institute of Radio Astronomy (Ukraine).

An example of the multi-look SAR image built without autofocus is shown in Fig. 11(a). One can observe significant defocusing. The reason of such effect is the presence of an uncompensated residual phase error.

An example of the application of the developed autofocus method based on the range-Doppler processing modified for short-time intervals is illustrated in Fig. 11(b). One can see that the SAR image is well focused which proves the efficiency of the developed autofocus algorithm.

V. Conclusions

In this paper we have demonstrated two important modifications of the well-known range-Doppler SAR processing algorithm.

First, the usage of multi-look processing in the range-Doppler domain with the extended Doppler bandwidth allows to account the existing antenna beam variations and perform the correction of radiometric errors. Another novel modification of the range-Doppler algorithm is intended for the formation of SAR images from the data collected on the

a

b

Fig. 11. Illustration of autofocusing results (a – SAR image before autofocus, b – SAR image after autofocus)

short-time intervals for the local quadratic phase error estimation, which is one of the key steps of the developed autofocus algorithm. Experimental results have shown the high efficiency of the developed methods in the combination with the modified range-Doppler algorithms.

References

[1] C. Oliver and S. Quegan, Understanding Synthetic Aperture Radar Images. Norwood, MA: Artech House, 1999.

[2] G. Franceschetti and R. Lanari, Synthetic Aperture Radar Processing. CRC Press, 1999.

[3] W. G. Carrara, R. S. Goodman, and R. M. Majewski, Spotlight Synthetic Aperture Radar: Signal Processing Algorithms. Boston; London: Artech House, 1995.

[4] I. G. Cumming and F. H. Wong, Digital Processing of Synthetic Aperture Radar Data: Algorithms and Implementation". Norwood, MA: Artech House, 2005.

[5] D.M. Vavriv et. al., "Cost-effective Ku band airborne SAR with Doppler centroid estimation, autofocusing and indication of moving targets", Proc. 2nd European Radar Conf. EuRAD2005, pp. 21-24, 2005.

[6] V.C. Koo et al., "A new unmanned aerial vehicle synthetic aperture radar for environmental monitoring", Progress in Electromagnetics Research, Vol. 122, pp. 245-268, 2012.

[7] D.M. Vavriv et al., "X-band SAR system for light-weight aircrafts", Proc. 15th Int. Radar Symp. IRS-2014, Gdansk, Poland, pp. 501-505, 2014.

[8] O.O. Bezvesilniy, I.M. Gorovyi and D.M. Vavriv, "Effects of local phase errors in multi-look SAR images", Progress In Electromagentics Research B, Vol. 53, pp. 1-24, 2013.

[9] O.O. Bezvesilniy, I.M. Gorovyi, V.V. Vynogradov and D.M. Vavriv, "Range-Doppler algorithm with extended number of looks", in Proc. Of 3rd Int. Microwaves, Radar and Remote Sensing Symp. MRRS 2011 (Kyiv, Ukraine), pp. 203-206, 2011.

[10] R. Bamler, "A comparison of range-Doppler and Wavenumber Domain SAR focusing algorithms ", IEEE Trans. On Geoscience and Remote Sensing, Vol. 30, No. 4, pp. 706-713, 1992.

[11] O.O. Bezvesilniy, I.M. Gorovyi, V.V. Vinogradov and D.M. Vavriv, "Multi-look radiometric correction of SAR images", Radiophysics and Radioastronomy, Vol. 16, No. 4, pp. 424-432, 2011.

[12] P. Samczynski and K. Kulpa, "Coherent MapDrift technique", IEEE Trans. on Geoscience and Remote Sensing, vol. 48, no. 3, pp. 1505–1517, 2010.

[13] I.M. Gorovyi, O.O. Bezvesilniy and D.M. Vavriv, "A novel trajectory restoration algorithm for high-resolution SAR imaging", Proc. 15th Int. Radar Symp. IRS-2014, Gdansk, Poland, pp. 170-173, 2014.

[14] O.O. Bezvesilniy, I.M. Gorovyi and D.M. Vavriv, "Estimation of phase errors in SAR data by local-quadratic map-drift autofocus" Proc. 13th Int. Radar Symp. IRS-2012, Warsaw, Poland, pp. 376-381, 2012.